toxics

MDPI

Article

Study on the Simultaneous Immobilization of Soluble Phosphorus and Fluorine in Phosphogypsum Using Activated Red Mud: Mechanism and Process Optimization

Yi Wang [1,*], Yanhong Wang [1], Guohua Gu [1,*] and Xuewen Wang [2]

[1] School of Minerals Processing and Bioengineering, Central South University, Changsha 410083, China
[2] School of Metallurgy and Environment, Central South University, Changsha 410083, China
* Correspondence: wangyiarticle123@163.com (Y.W.); guguohua@126.com (G.G.)

Abstract

Phosphogypsum (PG) is a byproduct of wet-process phosphoric acid production and contains soluble phosphorus (P), fluorine (F), and other harmful impurities in addition to calcium sulfate. Its acidic leachate enriched with P and F poses long-term risks to soil and surrounding water bodies. Owing to the incorporation of soluble P and F within calcium sulfate crystal interlayers, these contaminants are gradually released during storage, making it difficult to achieve an economically efficient and environmentally benign treatment of PG at an industrial scale. In this study, a low-cost and sustainable process for the effective and long-term immobilization of soluble P and F in PG was developed using sulfuric acid-activated red mud (RM), an industrial waste rich in Fe and Al. After pulping PG with water, activated RM was added, followed by pH adjustment with $Ca(OH)_2$, leading to the in situ formation of amorphous calcium aluminate and calcium ferrite polymers with strong adsorption affinity toward soluble P and F. The immobilization mechanism and phase evolution were systematically investigated using inductively coupled plasma optical emission spectroscopy (ICP-OES, PS-6PLASMA SPECTROVAC, BAIRD, USA), on a Rigaku Miniflex diffractometer (Rigaku Corporation, Tokyo, Japan), scanning electron microscopy coupled with energy-dispersive spectroscopy (SEM-EDS), and zeta potential analysis. The leachate of PG treated with activated RM and $Ca(OH)_2$ contained P < 0.5 mg/L and F < 10 mg/L at pH 8.5–9.0, meeting environmental requirements (pH = 6–9, P $\leq$ 0.5 mg/L, F $\leq$ 10 mg/L). Moreover, the immobilized P and F exhibited enhanced stability during long-term stacking, indicating the formation of durable immobilization products. This study demonstrates an effective "treating waste with waste" strategy for the large-scale, environmentally safe utilization of phosphogypsum.

Keywords: phosphogypsum; soluble P and F; red mud; immobilization; process optimization

Check for updates

Academic Editor: Roberto Rosal

Received: 24 December 2025
Revised: 19 January 2026
Accepted: 23 January 2026
Published: 2 February 2026

Copyright: © 2026 by the authors. Licensee MDPI, Basel, Switzerland. This article is an open access article distributed under the terms and conditions of the Creative Commons Attribution (CC BY) license.

1. Introduction

Phosphogypsum (PG) is a byproduct generated during the wet-process production of phosphoric acid, with approximately 4.5–5 tons of PG produced per ton of phosphoric acid [1,2]. Owing to the large-scale production and complex composition of PG, its global annual output has reached nearly 280 million tons, and the cumulative stockpiled amount has exceeded 6 billion tons worldwide, including more than 600 million tons in China alone [3]. PG mainly consists of $CaSO_4 \cdot 2H_2O$ (~90%), while the remaining fraction contains soluble phosphorus (P) and fluorine (F), silicates, organic additives, insoluble residues such as quartz, and trace heavy metals [4,5]. At present, storage remains the primary disposal

method for PG, and the presence of soluble P and F severely restricts its direct utilization as gypsum, resulting in a global comprehensive utilization rate of less than 20%.

During long-term storage, PG continuously releases acidic leachate with a pH ranging from 1.7 to 3.5 and containing high concentrations of soluble P and F, which poses persistent risks to soil and surrounding water bodies. Consequently, the development of economically viable and environmentally safe treatment technologies for PG has become a critical issue for the phosphorus industry. Numerous studies have investigated the removal or immobilization of soluble P and F in PG. Conventional approaches mainly include water washing and lime neutralization, which can remove a large fraction of soluble P and F but fail to achieve complete detoxification [6,7]. Even after repeated washing with fresh water, the residual concentrations of P and F in the washing effluent often exceed regulatory discharge limits.

$$Ca(OH)_2 \rightleftharpoons Ca^{2+} + 2OH^- \quad (1)$$

$$HF \rightleftharpoons H^+ + F \quad (2)$$

$$Ca^{2+} + 2F^- \rightleftharpoons CaF_2 \downarrow \quad (3)$$

$$Ca^{2+} + HPO_4{}^{2-} \rightleftharpoons CaHPO_4 \downarrow \quad (4)$$

$$H^+ + OH^- \rightleftharpoons H_2O \quad (5)$$

Lime neutralization is widely applied to precipitate soluble P and F in PG leachate, forming CaF_2 and $CaHPO_4$ according to Equations (1)–(5) [8–10]. However, due to the solubility limitations of CaF_2 and $CaHPO_4$, the residual concentrations of P and F in the leachate remain above the environmental requirements ($P \leq 0.5$ mg/L, $F \leq 10$ mg/L) within the practical pH range of 6–9. To overcome this limitation, combined methods involving $CaCO_3$ and $Al(OH)_3$ with mechanical ball milling have been proposed and shown to effectively immobilize soluble P and F in PG [11]. Nevertheless, the enormous quantity of PG makes such high-energy, mechanically intensive processes impractical for large-scale industrial application.

In environmental engineering, soluble aluminum and iron salts, such as polyaluminum chloride and polyferric sulfate, are commonly used as phosphorus removal agents [12] through the formation of aluminum and iron phosphate precipitates. Meanwhile, owing to the similarity in outer electron configuration between OH^- and F^-, hydroxyl groups in Al- and Fe-containing compounds can be partially substituted by F^-, enabling effective fluorine immobilization, as exemplified by $Al(OH)_3$-based materials. In recent years, crystalline calcium aluminate and calcium ferrite polymers have attracted considerable attention in materials science, particularly regarding their synthesis and structural regulation [13–15]. These crystalline phases have demonstrated promising performance in environmental applications, including phosphorus and fluorine removal [12,16,17]. In contrast, amorphous calcium aluminate and calcium ferrite polymers, which serve as precursors to their crystalline counterparts, have received comparatively limited attention, especially regarding their formation under mild conditions and their immobilization potential.

Red mud (RM) is an alumina refinery byproduct characterized by high alkalinity and enriched in iron and aluminum oxides [18,19]. Several studies have explored the direct use of untreated RM for immobilizing soluble P and F in PG [20]. However, such approaches typically require RM additions comparable to or exceeding the mass of PG, resulting in low utilization efficiency of Fe and Al, high transportation costs, and limited industrial feasibility due to the spatial separation of PG and RM sources. Previous studies have shown that sulfuric acid can effectively activate RM by converting solid-phase Al and Fe into soluble species [21,22], thereby substantially enhancing their reactivity and utilization efficiency.

These findings suggest that if RM is used as a soluble Al and Fe source to form calcium aluminate and calcium ferrite polymers, the immobilization efficiency of soluble P and F in PG can be significantly improved while drastically reducing RM consumption. Furthermore, achieving effective immobilization through the in situ formation of amorphous calcium aluminate and calcium ferrite polymers under ambient conditions, without high-temperature treatment, would offer a cost-effective and industrially attractive solution.

The objective of this study is to develop a low-cost, scalable, and environmentally sustainable process for the simultaneous immobilization of soluble phosphorus and fluorine in phosphogypsum. Specifically, sulfuric acid-activated red mud is employed as a soluble aluminum and iron source to generate amorphous calcium aluminate and calcium ferrite polymers under ambient conditions, thereby enabling efficient and long-term immobilization of P and F in PG without high-temperature treatment or mechanical activation.

This work aims to (i) elucidate the immobilization mechanism of soluble P and F via amorphous calcium aluminate and calcium ferrite polymers formed from activated RM and $Ca(OH)_2$, (ii) clarify the advantages of this approach over conventional methods relying on large quantities of untreated RM or energy-intensive ball milling processes, and (iii) evaluate the feasibility of reducing RM consumption to a small fraction of PG mass while ensuring long-term environmental stability. By addressing both mechanistic understanding and practical engineering constraints, this study provides a "treating waste with waste" strategy for the safe, large-scale management of phosphogypsum.

2. Materials and Methods

2.1. Materials

The reagents used in this study include sodium hydroxide (NaOH), calcium hydroxide ($Ca(OH)_2$), aluminum sulfate heptahydrate ($Al_2(SO_4)_3{\cdot}7H_2O$), ferric sulfate hydrate ($Fe_2(SO_4)_3{\cdot}H_2O$), disodium hydrogen phosphate (Na_2HPO_4), sodium fluoride (NaF), and sodium silicate nonahydrate ($Na_2SiO_3{\cdot}9H_2O$), all supplied by Sinopharm Chemical Reagent Co., Ltd. (Shanghai, China). Sulfuric acid (H_2SO_4, 98%) was also used. All reagents were of analytical grade (AR).The PG used in the study was obtained from Guizhou Kailin Group Public Co., Ltd. (Guizhou China). Table 1 shows the main components of RM from the China Aluminum Shandong Branch, which was washed, dried, and crushed to a 42 μm particle size before use.

Table 1. Chemical composition of RM, wt.%.

Al_2O_3	CaO	SiO_2	Na_2O	Fe_2O_3	TiO_2	K_2O	Loss on Ignition
22.42	3.32	16.33	8.72	33.82	5.55	0.25	9.37

Simultaneous Immobilization Flow Sheet of Soluble P and F in PG

Figure 1 shows the process flow sheet of the simultaneous immobilization of soluble P and F in PG, including two main steps: PG washing—washing water treatment and washed PG immobilizing. The PG washing was performed by stirring PG with water and filtering. The washed solution was neutralized with $Ca(OH)_2$ to precipitate P and F. The neutralized liquid was returned to the PG washing process.

On the other hand, the washed PG was immobilized with different agents, including $Ca(OH)_2$, soluble Fe or Al agents, and activated RM. The product was then filtered to obtain immobilized PG, and the filtrate was recycled for use in the immobilizing process.

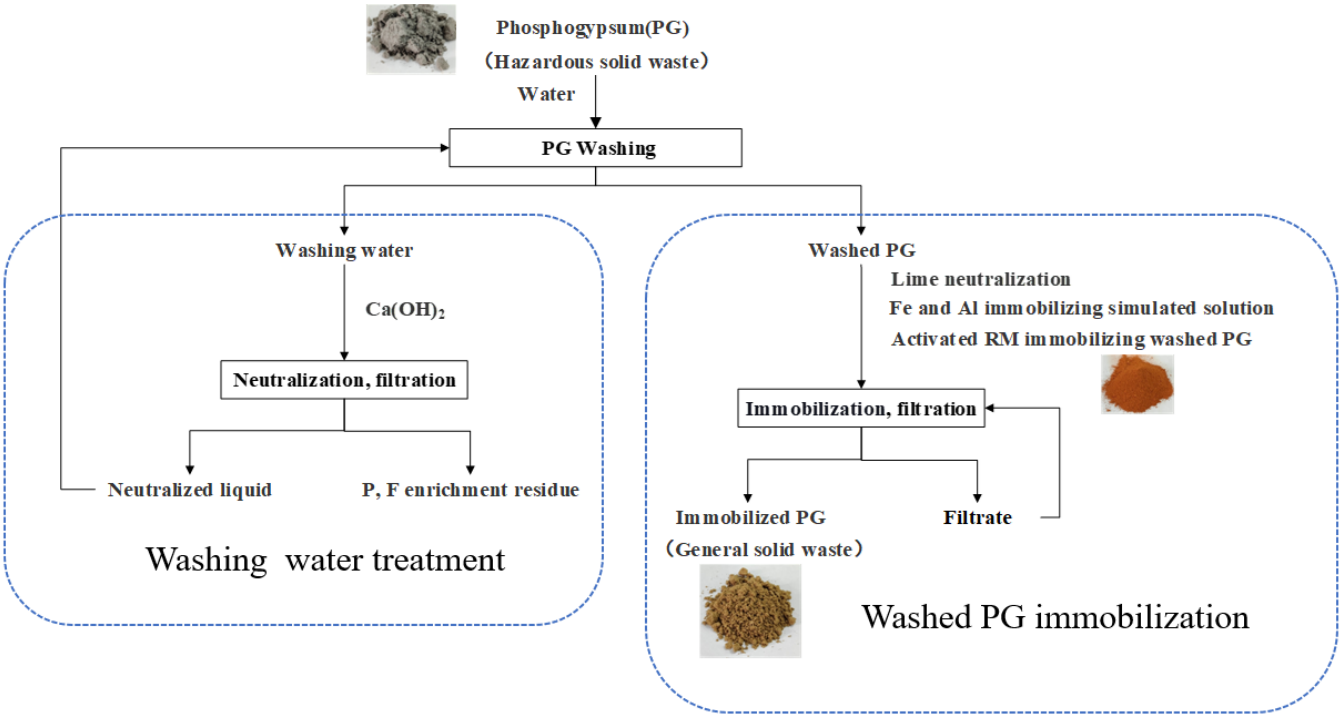


Figure 1. Process flow of harmless treatment for PG.

2.2. Experimental Design

2.2.1. PG Washing—Washing Water Treatment

PG washing was carried out to release soluble phosphorus (P) and fluorine (F) into the aqueous phase prior to subsequent immobilization. This part focuses on P and F removal from PG washing water. PG was mixed with water at a solid–liquid ratio of 1:1 (g/mL) and stirred at 400 rpm at room temperature. The effect of stirring time on the release of soluble P and F was investigated under otherwise identical conditions.

To evaluate the influence of repeated washing, PG was washed successively with fresh water at the same solid–liquid ratio. After each washing cycle, the slurry was filtered, the filtrate was collected for analysis, and the filter cake was reused for the next washing step. The washing effluent was then adjusted to pH 6–9 using $Ca(OH)_2$ to precipitate soluble P and F, and the neutralized liquid was recycled as washing water.

2.2.2. Washed PG Immobilization

After washing, a portion of soluble phosphorus (P) and fluorine (F) remained associated with the washed phosphogypsum. This part focuses on the immobilization of residual soluble P and F in the washed PG solid. Washed PG was mixed with water at a solid–liquid ratio of 1:1 (g/mL), and different immobilization agents were added under stirring at room temperature to evaluate their effectiveness in reducing P and F leachability.

Lime neutralization: The washed PG lime neutralization effect was obtained by adding washed PG to fresh water at a 1:1 g/mL S/L ratio and adding different amounts of $Ca(OH)_2$ to adjust the pH, followed by stirring at 400 rpm at room temperature for 3 h to achieve pH stabilization.

Fe and Al immobilizing simulated solution: A NaF and Na_2HPO_4 solution containing F 200 mg/L and P 30 mg/L was used to simulate the solution after the second PG wash. An amount of 3.6 g $Al_2(SO_4)_3{\cdot}7H_2O$ or 3 g $Fe_2(SO_4)_3{\cdot}H_2O$ was added to 200 mL simulated solution, then the pH was gradually adjusted with NaOH or $Ca(OH)_2$ to immobilize P and F at room temperature and the solution stirred at 400 rpm for 3 h. Due to PG containing soluble Si, 5 g $Na_2SiO_3{\cdot}9H2O$ was added to 200 mL simulated solution, and the pH was

adjusted to 2 with H_2SO_4. Then, the experiments above were repeated to investigate the effect of SiO_3^{2-} on the removal of F by soluble Fe and Al. To further study the effect of soluble Si on F in solution without Fe and Al elements, 5 g $Na_2SiO^3 \cdot 9H2O$ was added to 200 mL simulated solution and the solution adjusted to different pH values with H_2SO_4 keeping the other conditions the same. The immobilizing effect of Fe and Al was assessed by simultaneously adding 1.8 g $Al_2(SO_4)_3 \cdot 7H_2O$ and 1.5 g $Fe_2(SO_4)_3 \cdot H_2O$ to 200 mg/L simulated solution and adjusting the pH with $Ca(OH)_2$ while keeping the other conditions the same.

Activated RM immobilizing washed PG: The activated RM was obtained by adding RM to water at an S/L ratio of 1:1.5 g/cm under stirring and then slowly adding 98% H_2SO_4. After stirring the slurry at ~95 °C for 40 min, the activation of RM was completed. The immobilization includes mixing 6 g of activated RM with 200 g washed PG and water at a 1:1 g/mL S/L ratio and adjusting the pH with $Ca(OH)_2$, followed by stirring at 400 rpm at room temperature for 3 h. To determine the amount of H_2SO_4 required for activation, 6 g RM was activated with different doses of H_2SO_4 and used to immobilize 200 g washed PG at pH 9. Then, 6 g RM, activated by 12 g H_2SO_4, was used to immobilize 200 g washed PG, whereas the blank experiment used only $Ca(OH)_2$ to adjust the pH without adding activated RM. The immobilization effect of activated RM and the immobilized supernatant's zeta potential were measured.

2.3. Analysis Methods

The phosphorus (P) concentration in experimental samples was determined using inductively coupled plasma optical emission spectroscopy (ICP-OES, PS-6PLASMA SPECTROVAC, BAIRD, Wisconsin, WI, USA), and fluorine (F) was measured using a fluoride ion-selective electrode (PF-1, Kangyi Instrument Ltd., Langfang, China). The surface morphology of treated phosphogypsum was examined using an ultra-high-resolution field emission scanning electron microscope (SEM, CLARA with EDS, TESCAN, Brno, Czech Republic). X-ray diffraction (XRD) patterns were recorded on a Rigaku Miniflex diffractometer with Cu Kα radiation operated at 35 kV and 20 mA to identify phase composition before and after immobilization. Zeta potential measurements were conducted using a Nano ZS90 analyzer (Malvern Instruments Ltd., Malvern, UK) to evaluate the surface charge characteristics of the suspension during immobilization and to support the analysis of P and F adsorption behavior; measurements were performed on the supernatant after pH adjustment under identical conditions.

The environmental performance of immobilized PG was evaluated according to the Chinese national standard GB 18599-2020 (Standard for pollution control on the non-hazardous industrial solid waste storage and landfill). For leaching tests, 5 g of immobilized PG was mixed with 50 mL of ultrapure water in a polyethylene bottle, shaken at 110 r/min at room temperature for 8 h, and allowed to stand for 16 h. The filtrate obtained after filtration was analyzed, and PG was classified as general solid waste only when the leachate met the criteria of pH = 6–9, P $\leq$ 0.5 mg/L, and F $\leq$ 10 mg/L. All immobilized PG samples in this study were evaluated using this method.

3. Results and Discussion

3.1. PG Washing—Washing Water Treatment

The experimental results of PG washed with water are shown in Figure 2. Figure 2a shows the relationship between the concentrations of P and F in washing water and stirring time. As can be seen from the figure, the dissolution rate of P in PG was faster than that of soluble F under the same conditions. After stirring for 1 h, the dissolution of both P and F reached an equilibrium state.

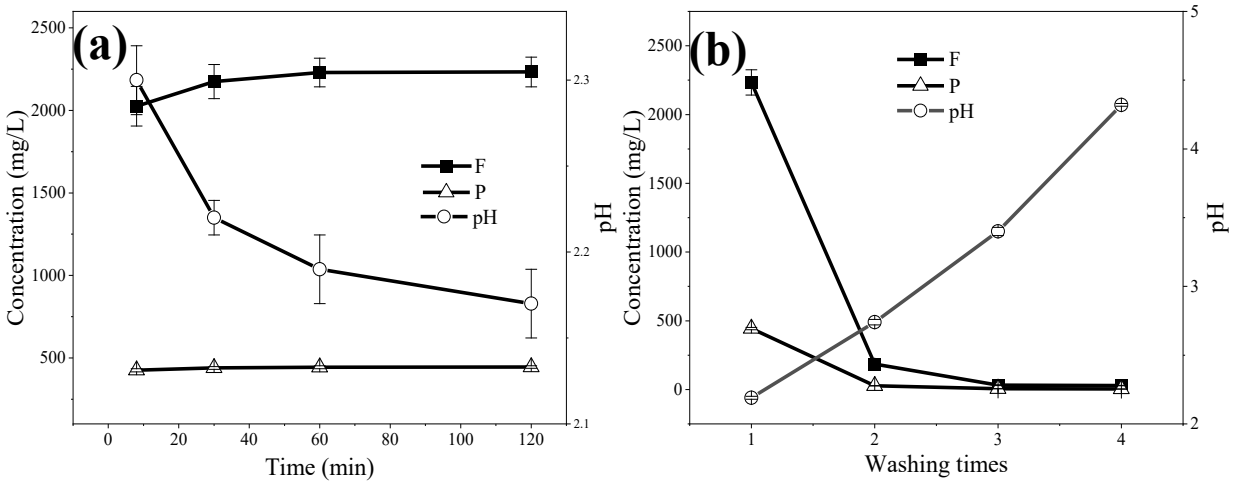


Figure 2. Experimental results of PG washed with water: (**a**) the influence of stirring time on washing effect; (**b**) the effect of repeated washing with fresh water.

Figure 2b shows the effect of repeat washing of PG with fresh water on the pH and the concentration of P and F in the washing water. The pH of the washing water gradually increased as the number of washes increased. The first water wash removed more than 90% of soluble P and F in PG. The contents of P and F in the washing water showed a cliff-like decrease after the first washing. The contents of P and F in the following rounds slowly decreased in sequence, and the magnitude of the decrease became smaller and smaller. The concentrations of P and F in the water after the fourth wash were 4 mg/L and 29 mg/L, respectively. Hence, washing PG with water alone cannot meet the environmental requirements for P $\leq$ 0.5 mg/L and F $\leq$ 10 mg/L.

The concentrations of P and F in the water from the first wash were 443.5 mg/L and 2233 mg/L, respectively, with separation and recovery values. Table 2 shows the chemical compositions of PG before and after one wash. When the washing water was neutralized to pH 8.9 with $Ca(OH)_2$, the soluble P and F transferred into CaF_2 and $CaHPO_4$, as introduced in Equations (1)–(5), which resulted in 3 mg/L and 35 mg/L soluble P and F left in the solution, respectively. The neutralized liquid was reused for PG washing. Table 3 lists the main components of the P and F enrichment residue after neutralization. The average content of P and F was 4.4 wt.% and 10.7 wt.%, respectively. This P and F can be reused as raw materials to produce wet-process phosphoric acid.

Table 2. Chemical composition of PG before and after washing, wt.%.

	CaO	SO_3	SiO_2	P_2O_5	F	Fe_2O_3	Al_2O_3	Na_2O
Before	38.24	53.01	5.66	1.14	0.50	0.30	0.53	0.18
After	38.87	54.16	4.52	1.01	0.22	0.31	0.42	0.03

Table 3. Main components of P- and F-enriched residues, wt.%.

P	F	Si	Ca
4.4	10.7	5.16	36.9

3.2. Washed PG Immobilization

3.2.1. Lime Neutralization

After washing once, a portion of the soluble P and F remained in the washed PG. Lime neutralization is a common method to reduce soluble P and F in PG. Figure 3 shows the results of lime neutralization for washed PG. The concentration of F and P in the leaching

solution decreased with the increase in pH. However, the concentration of F was about 30 mg/L and the concentration of P exceeded 0.5 mg/L at pH 6~9 in the PG filtrate, which does not meet the environmental standards. After lime treatment, the main component of PG is $CaSO_4$, and the residual soluble P and F in PG are present as $Ca(H_2PO_4)_2$, $CaHPO_4$, and CaF_2, respectively [23]. The lime-neutralized solution is a saturated solution of $CaSO_4$. The Ksp of $CaSO_4$ is 9.1×10^{-6}, with 3×10^{-3} mol/L Ca^{2+} in the solution, while the Ksp of CaF_2 is 5.3×10^{-9}, with 25 mg/L F- in the saturated solution of $CaSO_4$ via the dissolving of CaF_2. Similarly, the Ksp of $Ca(H_2PO_4)_2$ and $CaHPO_4$ also led to P > 0.5 mg/L at pH 6~9. Hence, the Ksp of $Ca(H_2PO_4)_2$, $CaHPO_4$, and CaF_2 determined that the lime neutralization cannot remove F and P to the extent necessary to meet environmental requirements.

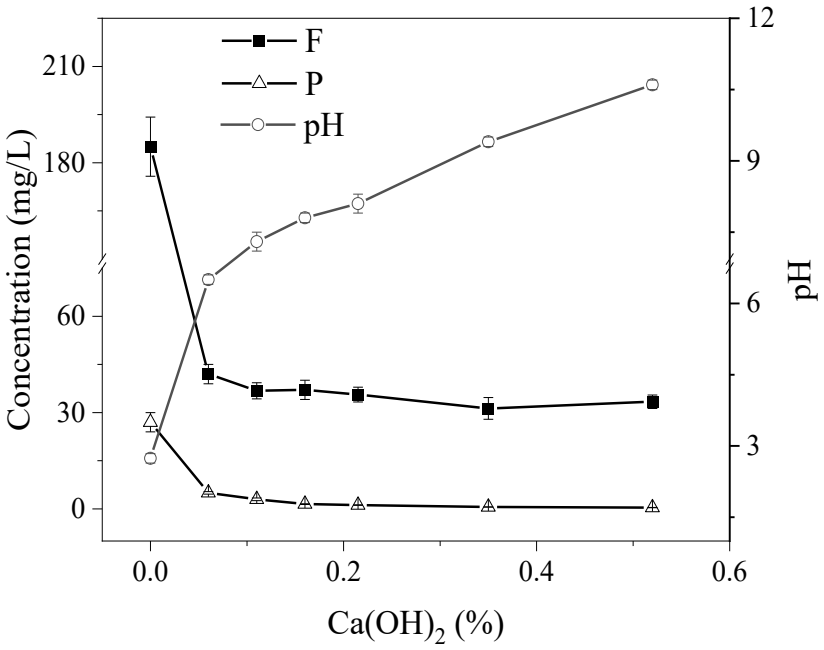


Figure 3. The F and P concentration in the solution of lime-treated PG.

3.2.2. Comparative Immobilization of P and F Using Soluble Al and Fe Salts

The above study indicates that neither water-washed nor lime-neutralized PG can meet environmental protection requirements. Nevertheless, the first washing solution can be recovered. To further immobilize the soluble P and F in the second washing solution, NaF and Na_2HPO_4 were used to prepare the simulated solution for the second wash. In subsequent experiments, Fe and Al compounds were used to immobilize the soluble P and F in the simulated solution.

Figure 4 shows the experimental results of adding $Al_2(SO_4)_3 \cdot 7H_2O$ or $Fe_2(SO_4)_3 \cdot H_2O$ into the simulated solution and using NaOH or $Ca(OH)_2$ to adjust the pH. The content of P and F in the solution decreased with the increase in pH from acidic to neutral. In Figure 4(a1), when using $Al_2(SO_4)_3 \cdot 7H_2O$ and NaOH, the P, F, and Al in the simulation solution first decreased and then increased as the pH increased above 8. The solution became transparent when the precipitate dissolved completely at pH > 12. When using $Al_2(SO_4)_3 \cdot 7H_2O$ and $Ca(OH)_2$ in Figure 4(a2), the P and F removal effect was better than using $Al_2(SO_4)_3 \cdot 7H_2O$ and NaOH. The Al and F in the solution slightly increased at pH 8–10. Then, when the pH was further increased to above 10, F kept decreasing. In Figure 4(b1), when using $Fe_2(SO_4)_3 \cdot H_2O$ and NaOH, the F in the simulation solution first decreased and then increased with the increase in pH, similar to but worse than using $Al_2(SO_4)_3 \cdot 7H_2O$ and NaOH. P < 0.5 mg/L at pH > 5. When using $Fe_2(SO_4)_3 \cdot H_2O$ and $Ca(OH)_2$ in Figure 4(b2), the F removal effect was significantly better than using

$Fe_2(SO_4)_3 \cdot H_2O$ and NaOH. The F concentration was 7.8 mg/L and P exceeded 0.5 mg/L at pH 7. As the pH continued to increase, the F content further decreased. This means the reaction of $Al_2(SO_4)_3 \cdot 7H_2O$ and $Fe_2(SO_4)_3 \cdot H_2O$ with $Ca(OH)_2$ formed substances different from the reaction of $Al_2(SO_4)_3 \cdot 7H_2O$ and $Fe_2(SO_4)_3 \cdot H_2O$ with NaOH, which had a better F and P immobilization effect.

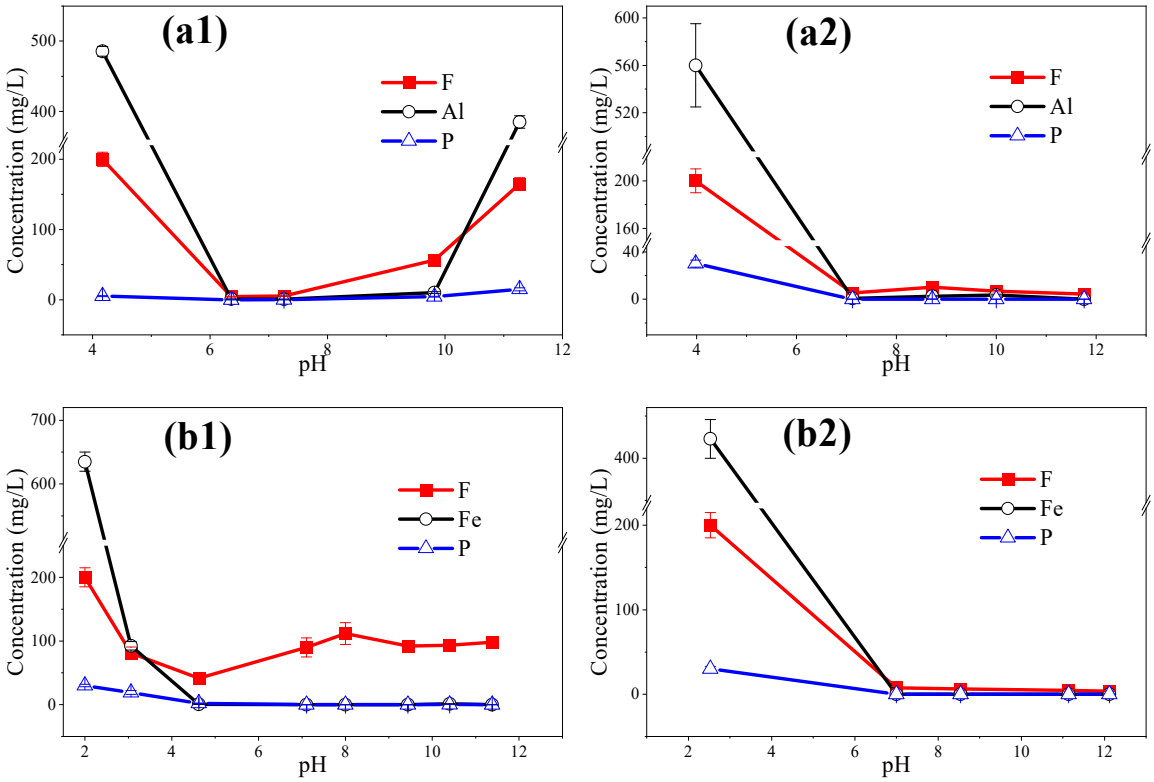


Figure 4. P and F immobilization from simulated solution: (**a1**) adding $Al_2(SO_4)_3 \cdot 7H_2O$ and NaOH; (**a2**) adding $Al_2(SO_4)_3 \cdot 7H_2O$ and $Ca(OH)_2$; (**b1**) adding $Fe_2(SO_4)_3 \cdot H_2O$ and NaOH; (**b2**) adding $Fe_2(SO_4)_3 \cdot H_2O$ and $Ca(OH)_2$.

PG contains soluble silicate. The effect of soluble silicon on P and F immobilization is shown in Figure 5, which shows the results of adding $Na_2SiO_3 \cdot 9H_2O$ to the simulated solution, adjusting pH to 2 with H_2SO_4 and then repeating the four experiments in Figure 4. Compared with Figure 4, the P removal effect did not change and the F removal trend was the same but the effect was worse.

To further study the effect of soluble Si on F in solution, Figure 6a shows the results of adding $Na_2SiO_3 \cdot 9H_2O$ to the simulated solution and adjusting the pH with H_2SO_4. F in the solution decreased with the decrease in pH. When the pH decreased to <9, precipitate began to appear; the lower the pH, the more precipitate formed. Figure 6b shows the results obtained by adding $Al_2(SO_4)_3 \cdot 7H_2O$ and $Fe_2(SO_4)_3 \cdot H_2O$ to simulated solution and adjusting the pH with $Ca(OH)_2$. It can be observed that after halving the dosage of $Al_2(SO_4)_3 \cdot 7H_2O$ and $Fe_2(SO_4)_3 \cdot H_2O$, the immobilizing effect obtained by mixing them was slightly better than using $Al_2(SO_4)_3 \cdot 7H_2O$ or $Fe_2(SO_4)_3 \cdot H_2O$ alone.

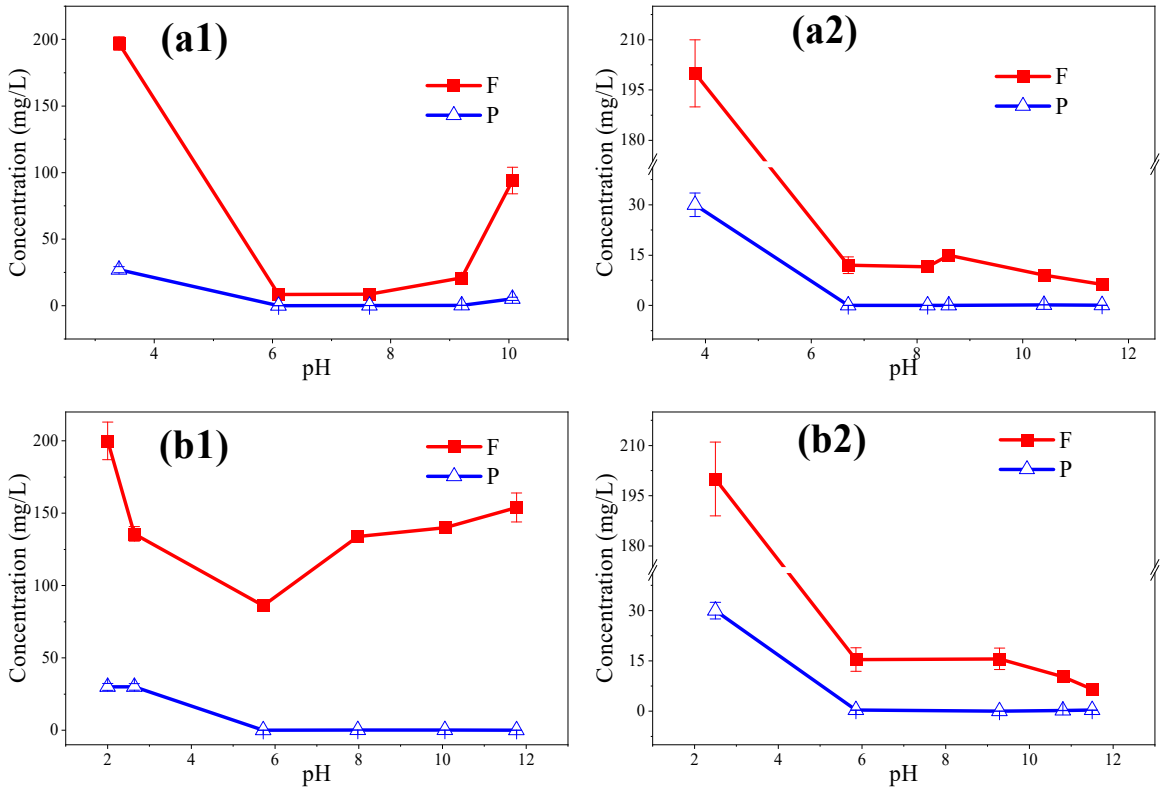


Figure 5. P and F immobilization from simulated solution: (**a1**) adding $Na_2SiO_3 \cdot 9H_2O$, $Al_2(SO_4)_3 \cdot 7H_2O$ and NaOH; (**a2**) adding $Na_2SiO_3 \cdot 9H_2O$, $Al_2(SO_4)_3 \cdot 7H_2O$, and $Ca(OH)_2$; (**b1**) adding $Na_2SiO_3 \cdot 9H_2O$, $Fe_2(SO_4)_3 \cdot H_2O$, and NaOH; (**b2**) adding $Na_2SiO_3 \cdot 9H_2O$, $Fe_2(SO_4)_3 \cdot H_2O$, and $Ca(OH)_2$.

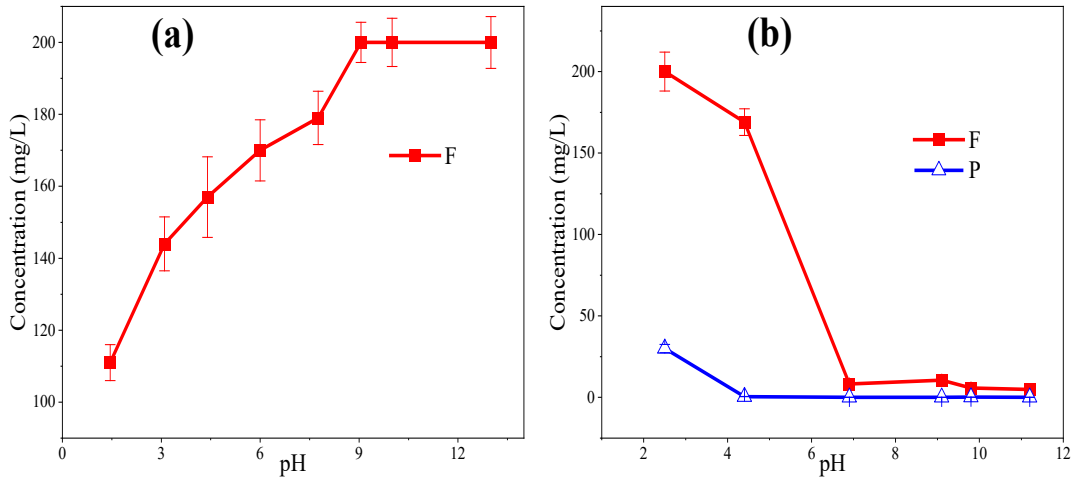


Figure 6. P and F immobilization from simulated solution: (**a**) adding $Na_2SiO_3 \cdot 9H_2O$ and H_2SO_4; (**b**) adding $Al_2(SO_4)_3 \cdot 7H_2O$, $Fe_2(SO_4)_3 \cdot H_2O$, and $Ca(OH)_2$.

Figure 6b presents the results obtained by adding $Al_2(SO_4)_3 \cdot 7H_2O$ and $Fe_2(SO_4)_3 \cdot H_2O$ to the simulated solution and adjusting the pH with $Ca(OH)_2$. It can be observed that, after halving the dosages of $Al_2(SO_4)_3 \cdot 7H_2O$ and $Fe_2(SO_4)_3 \cdot H_2O$, the immobilization effect achieved by their combined addition was slightly superior to that obtained using $Al_2(SO_4)_3 \cdot 7H_2O$ or $Fe_2(SO_4)_3 \cdot H_2O$ alone.

3.3. Activated RM Immobilizing Washed PG

The above results show that soluble Al and Fe with the addition of $Ca(OH)_2$ have a good immobilization effect on P and F. In fact, RM contains abundant Al and Fe, with 22.42% Al_2O_3 and 33.82% Fe_2O_3, as shown in Table 1. Hence, if RM can be activated with H_2SO_4 to convert Al and Fe into soluble species, it can serve as a low-cost agent for immobilizing soluble P and F in PG.

Figure 7 shows the experimental results obtained by activating RM with different doses of H_2SO_4 and immobilizing washed PG with $Ca(OH)_2$ at pH 9. As can be seen, with an increase in the H_2SO_4 dosage from 0 to 3 g, the P concentration in the leachate of immobilized PG decreased from 7 mg/L to 0.2 mg/L (<0.5 mg/L), while the F concentration decreased from 31 mg/L to 24.5 mg/L, indicating that activated RM preferentially immobilizes soluble P in PG. As the H_2SO_4 dosage further increased, the F concentration in the leachate continuously decreased, whereas P remained at a low level (<0.5 mg/L). When the H_2SO_4 dosage increased from 3 to 12 g, the F concentration decreased from 24.5 mg/L to 9.6 mg/L (<10 mg/L).

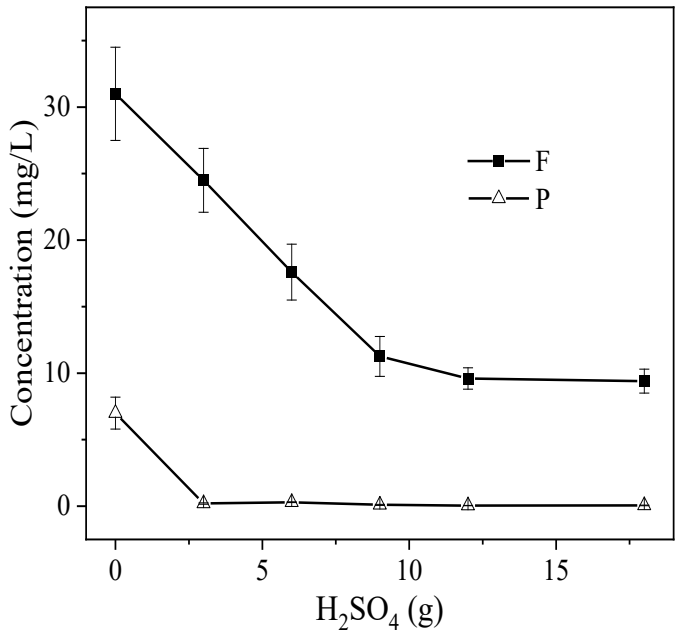


Figure 7. Immobilization effect of RM activated with different H_2SO_4 dosages.

Based on these results, the optimal weight ratio of H_2SO_4 to RM during activation should be $\geq$ 2, and the RM dosage required is approximately 3% of the PG mass to immobilize soluble P and F to meet the regulatory standards (P $\leq$ 0.5 mg/L, F $\leq$ 10 mg/L, and pH = 6–9).

Therefore, the RM required for PG treatment is only 3% of the PG mass, which significantly reduces treatment and reagent costs and is highly favorable for industrial implementation.

Figure 8 shows the experimental results obtained by using activated RM to immobilize washed PG and adjusting the pH with $Ca(OH)_2$; the blank experiment only used $Ca(OH)_2$ to adjust the pH without adding activated RM. The soluble F immobilization effect achieved by activated RM combined with $Ca(OH)_2$ was significantly better than that obtained using $Ca(OH)_2$ alone. With the addition of activated RM, the concentration of F decreased with increasing pH; when the pH increased to 8.9, the F concentration decreased to 9.6 mg/L (<10 mg/L), whereas it remained at 35 mg/L in the absence of activated RM.

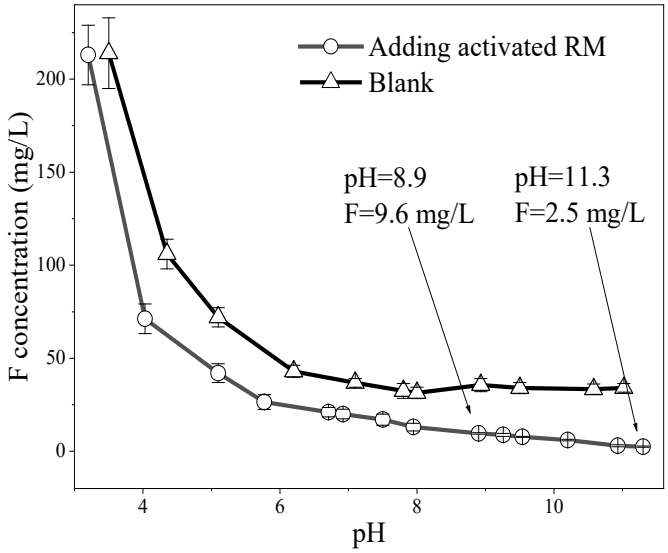


Figure 8. Effect of soluble F immobilization by activated RM and only using $Ca(OH)_2$.

The XRD patterns of PG before and after activated RM immobilization are shown in Figure 9, including both the main crystal phases $CaSO_4 \cdot 2H_2O$ and $CaSO_4 \cdot 0.5H_2O$; the crystal compositions before and after immobilization were basically the same. Figure 9b further indicates that the immobilization product of soluble Al and Fe from activated RM was amorphous.

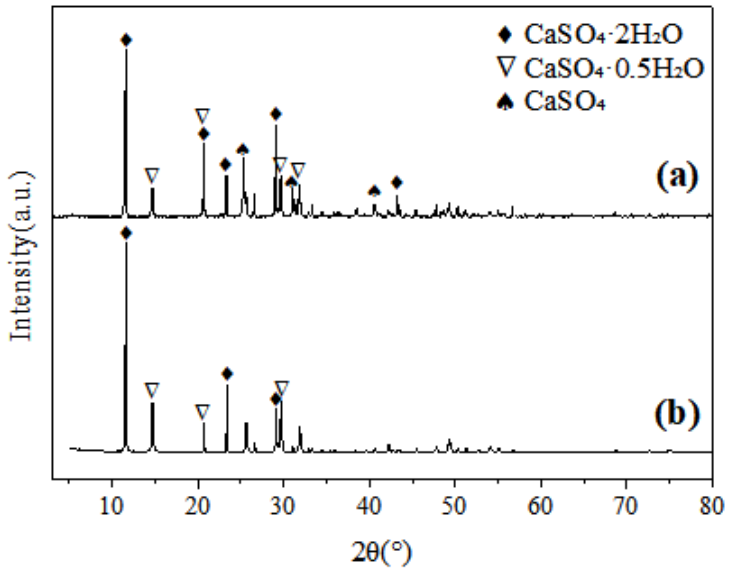


Figure 9. XRD patterns: (**a**) washed PG before immobilization; (**b**) washed PG immobilized with activated RM and $Ca(OH)_2$ at pH ~8.5.

3.4. Mechanism of P and F Removal

3.4.1. The Existence of Calcium Aluminate and Calcium Ferrite Polymers

Crystalline calcium aluminate and calcium ferrite polymers can be prepared by mixing soluble Fe and Al with Ca and heating [14,15]. As shown in Figure 9, the products formed by soluble Fe and Al with $Ca(OH)_2$ at room temperature are amorphous, exhibiting a good immobilization effect for P and F in the experiments shown in Figure 4.

To illustrate the existence of amorphous calcium aluminate and calcium ferrite polymers, $Al_2(SO_4)_3 \cdot 7H_2O$ and $Fe_2(SO_4)_3 \cdot H_2O$ were separately dissolved in water, and the pH was then adjusted to 12 using $Ca(OH)_2$. The resulting solutions were filtered to obtain the

solid residues, which were subsequently dried in an oven at 100 °C for 12 h. Figure 10 presents the XRD patterns of the dried samples.

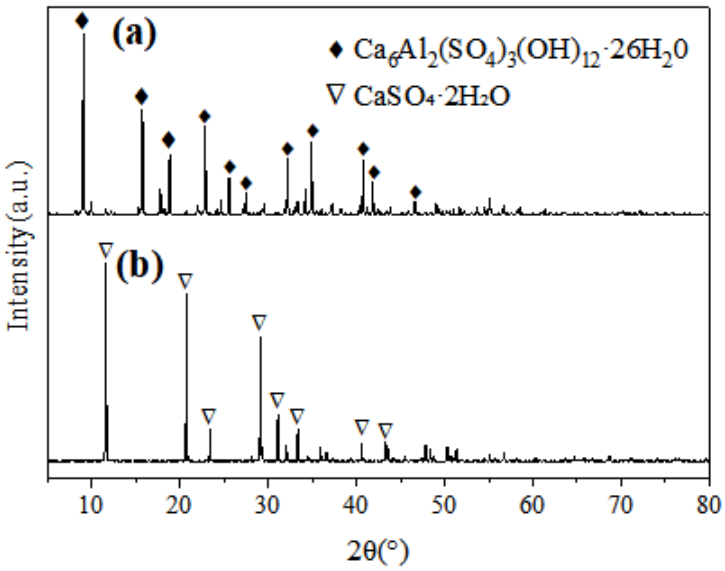


Figure 10. XRD pattern of experimental samples: (**a**) calcium aluminate polymer dried at 100 °C for 12 h; (**b**) calcium ferrite polymer dried at 100 °C for 12 h.

Figure 10a shows that the calcium aluminate polymer formed from soluble Al species and $Ca(OH)_2$ is a precursor of the crystalline phase $Ca_6Al_2(SO_4)_3(OH)_{12}\cdot 26H_2O$, which exhibits a strong adsorption capacity for F^- [17]. Figure 10b indicates that, even after drying at 100 °C, the calcium ferrite polymer remains amorphous. Conversion of the calcium ferrite polymer into crystalline phases requires higher temperatures [13,14,16].

Figure 11 shows the removal of P and F from 200 mL of simulated solution using $Ca_6Al_2(SO_4)_3(OH)_{12}\cdot 26H_2O$ powder, which was synthesized from 3.6 g $Al_2(SO_4)_3\cdot 7H_2O$ and $Ca(OH)_2$. By comparing Figure 4(a2) and Figure 11, it can be observed that the immobilization trends of P and F are consistent. At pH $\geq$ 8, the fluoride removal efficiency of $Ca_6Al_2(SO_4)_3(OH)_{12}\cdot 26H_2O$ was superior to that of the amorphous calcium aluminate polymer. Proper crystallization can therefore enhance the performance of fluoride removal materials.

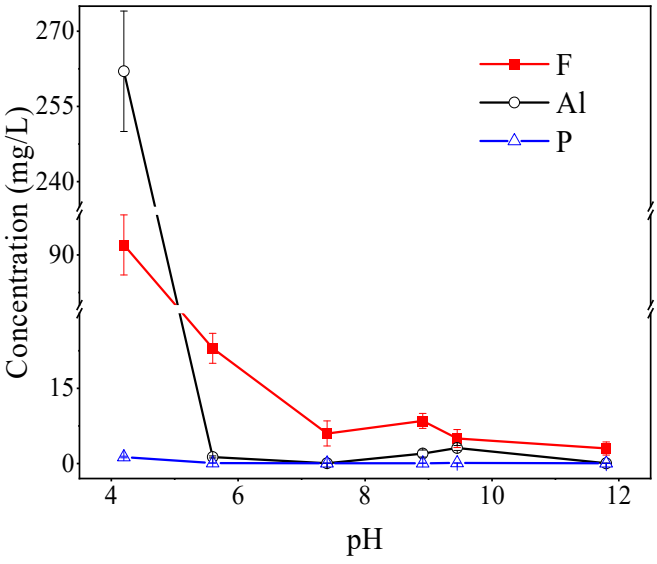


Figure 11. P and F immobilization from simulated solution by $Ca_6Al_2(SO_4)_3(OH)_{12}\cdot 26H_2O$.

A similar phenomenon is observed for $Al(OH)_3$ and activated alumina (γ-Al_2O_3 or χ-Al_2O_3) produced by thermal treatment of $Al(OH)_3$ [24]. Activated alumina exhibits stronger defluorination capability and lower solubility than $Al(OH)_3$ and is widely applied for fluoride removal from aqueous solutions in both industrial and domestic contexts [25].

3.4.2. Immobilization of P and F

Visual MINTEQ (version 3.0, KTH Royal Institute of Technology, Stockholm, Sweden) was used to calculate chemical speciation within the pH range of 0–14 (Figure 12). The initial temperature was 25 °C, and the concentrations of F and P were 185 mg/L and 27 mg/L, respectively, which are the same as those in the second washing solution of PG shown in Figure 2b. Figure 12 indicates that when the pH is in the range of 6–9, phosphorus mainly exists as $H_2PO_4^-$ and HPO_4^{2-}, whereas fluorine predominantly exists as F^-.

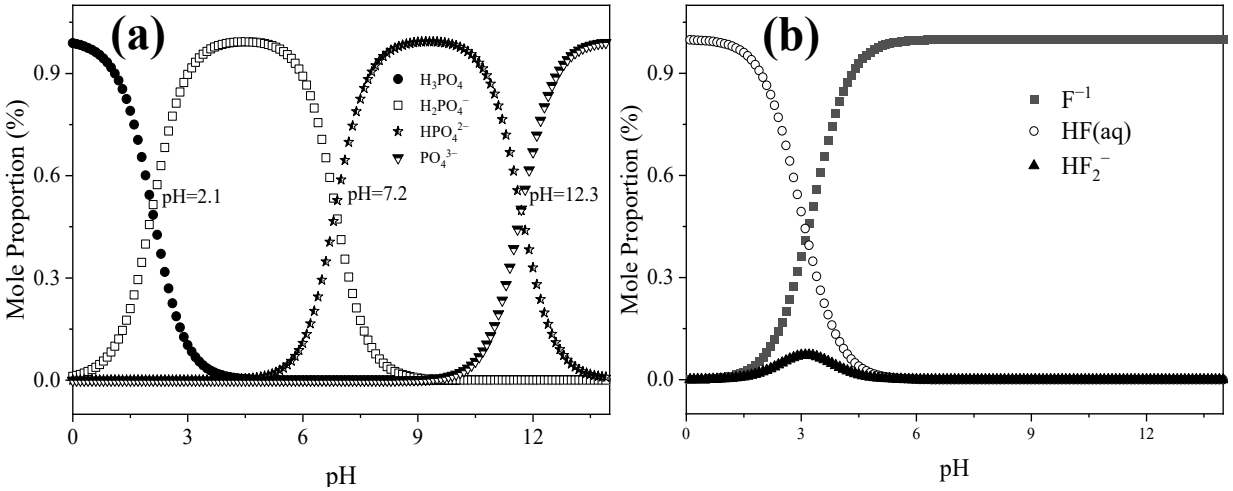


Figure 12. Influence of pH on the existing forms of ions: (**a**) phosphorus; (**b**) fluorine.

Based on the above experimental and simulation results, the following conclusions can be drawn. Figure 4 shows the experiments in which soluble Fe and Al were used to immobilize the simulated solution. When the pH was increased to above 4.2 using NaOH, PO_4^{3-} combined with Al^{3+} to form an $AlPO_4$ precipitate, while the remaining Al^{3+} precipitated as $Al(OH)_3$. F^- substituted for OH^- in $Al(OH)_3$ to form $Al(OH)_{(3-x)}F_x$, resulting in a defluorination effect. A molecular stick model is shown in Figure 13a.

When the pH increased to above 8.2, $AlPO_4$ and $Al(OH)_{(3-x)}F_x$ began to dissolve, and they were completely dissolved when the pH was further increased to 12 [26].

When the pH was increased using NaOH, $Fe_2(SO_4)_3{\cdot}H_2O$ exhibited a behavior similar to that of $Al_2(SO_4)_3{\cdot}7H_2O$ in the removal of P and F. When the pH increased to > 5, P precipitated as $FePO_4$, while the remaining Fe^{3+} precipitated as $Fe(OH)_3$. F^- substituted for OH^- in $Fe(OH)_3$ to form $Fe(OH)_{(3-x)}F_x$, producing a defluorination effect. A molecular stick model is shown in Figure 13b.

The removal of P and F using $Al_2(SO_4)_3{\cdot}7H_2O$ by adjusting the pH with $Ca(OH)_2$ was more effective than that achieved using NaOH. $Al(OH)_{(3-x)}F_x$ began to dissolve at pH values above 8.2, resulting in a slight increase in the concentrations of Al and F in the solution. Meanwhile, Al species reacted with $Ca(OH)_2$ to form calcium aluminate polymer precipitates capable of adsorbing F. A molecular stick model is shown in Figure 13c. As the pH increased, the amount of calcium aluminate polymer increased, and its adsorption capacity for F was enhanced, leading to a decrease in the F concentration in the solution.

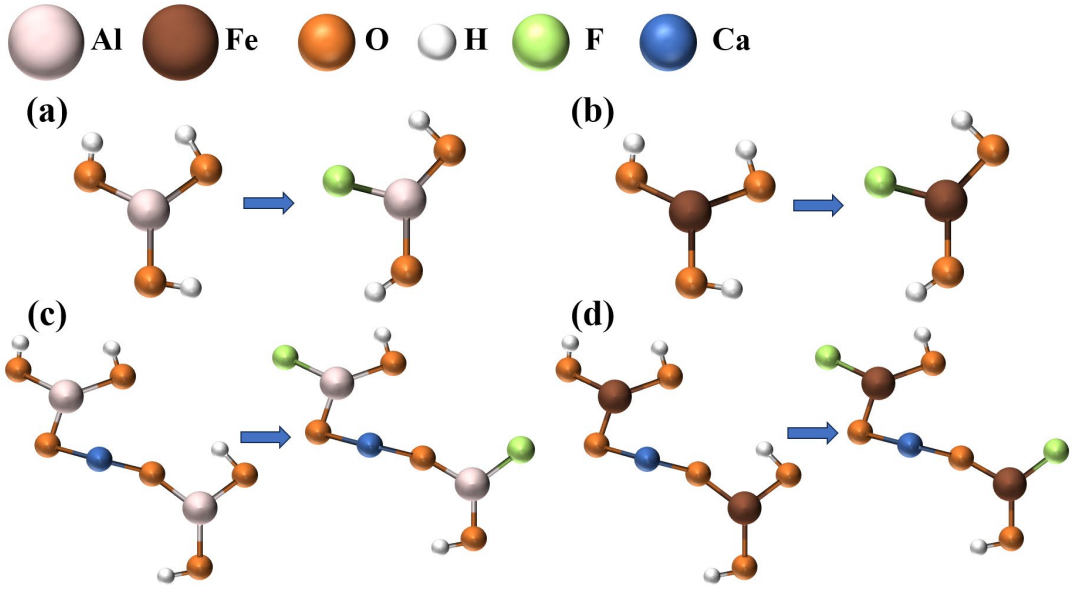


Figure 13. Molecular stick model of adsorption of F by Fe and Al compounds. (**a**) Substitution of hydroxyl groups by F^- in aluminum hydroxide, forming $Al(OH)_{(3-x)}F_x$; (**b**) Substitution of hydroxyl groups by F^- in iron hydroxide, forming $Fe(OH)_{(3-x)}F_x$; (**c**) Adsorption of F^- by amorphous calcium aluminate polymer formed from Al species and $Ca(OH)_2$; (**d**) Adsorption of F^- by amorphous calcium ferrite polymer formed from Fe species and $Ca(OH)_2$.

Similarly, the removal of P and F using $Fe_2(SO_4)_3{\cdot}H_2O$ by adjusting the pH with $Ca(OH)_2$ was also more effective than that using NaOH. Fe species reacted with $Ca(OH)_2$ to form calcium ferrite polymers capable of adsorbing F, as illustrated by the molecular stick model shown in Figure 13d. Aluminum sulfate and iron sulfate can therefore serve as reagents for the mixed immobilization of soluble P and F, and the combined application exhibits a slightly superior effect compared with the use of a single agent, indicating a synergistic effect between aluminum sulfate and iron sulfate in immobilizing soluble P and F. The following reaction Equations (6)–(11) represent the immobilization of soluble F and P in solution:

$$Al^{3+} + PO_4{}^{3-} = AlPO_4 \downarrow \quad (6)$$

$$Al_2(SO_4)_3 + 3Ca(OH)_2 = 3CaSO_4\downarrow + 3Al(OH)_3 \downarrow \quad (7)$$

$$Fe_2(SO_4)_3 + 3Ca(OH)_2 = 3CaSO_4\downarrow + 3Fe(OH)_3 \downarrow \quad (8)$$

$$Me(OH)_3 + xF^- = Me(OH)_{(3\text{-}x)}F_x + xOH^-, \text{ Me = Al, Fe} \quad (9)$$

$$nMe(OH)_3 + mCa(OH)_2 = Ca_mO_{2m}Me_n(OH)_{(3n-2m)} + 2mH_2O \quad (10)$$

$$Ca_mO_{2m}Me_n(OH)_{(3n-2m)} + yF^- = Ca_mO_{2m}Me_n(OH)_{(3n-2m-y)}F_y + yOH^- \quad (11)$$

When Si was present in the simulated solution and the pH was lower than 9, $SiO_2{}^{2-}$ began to precipitate to form $xSiO_2{\cdot}yH_2O$; the lower the pH, the greater the amount of $xSiO_2{\cdot}yH_2O$ formed. It is well known that $SiO_3{}^{2-}$ in solution has a chelating effect on F^-, and that $xSiO_2{\cdot}yH_2O$ can adsorb F^-. Consequently, the concentration of F^- increased with increasing $SiO_3{}^{2-}$ concentration, which explains why the addition of $Na_2SiO_3{\cdot}9H_2O$ resulted in a decrease in F removal efficiency when the pH increased to above 6 [25].

3.4.3. Mechanism and Stacking Effect of Activated RM Immobilizing Washed PG

Figure 8 shows the experiments using activated RM to immobilize washed PG, along with the blank experiment in which only $Ca(OH)_2$ was used to adjust the pH without adding activated RM. Figure 14 presents the corresponding zeta potential results. In the

blank experiment, Equations (1)–(5) predominantly occurred during pH adjustment with $Ca(OH)_2$. With the addition of $Ca(OH)_2$ alone, the pH increased from 3.5 to 6.4, and the zeta potential decreased from −3.5 mV to −24.5 mV. During this process, particles continuously adsorbed F^- onto their surfaces to form CaF_2, and the F concentration approached that of a CaF_2-saturated solution.

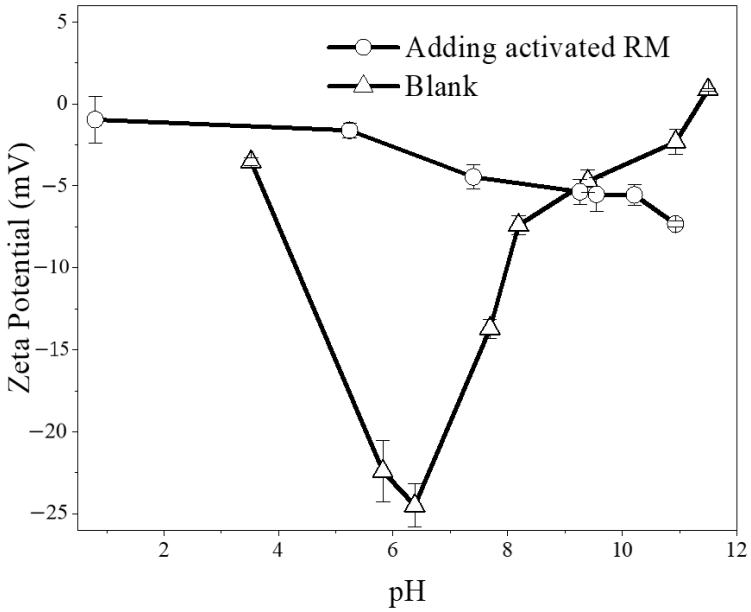


Figure 14. Zeta potential of soluble F immobilization by activated RM and only using $Ca(OH)_2$.

When the pH further increased from 6.4 to 11.5, the formation of CaF_2 no longer increased, the F concentration remained essentially unchanged, and the anion density on the particle surfaces no longer increased, resulting in an increase in zeta potential from −24.5 mV to 0.9 mV.

In contrast, when activated RM was added and the pH was adjusted using $Ca(OH)_2$, Equations (6)–(12) predominantly occurred in the solution without the formation of CaF_2. Instead, amorphous calcium aluminate and calcium ferrite polymers were formed, and their adsorption capacity for F increased with increasing pH. As a result, the concentration of F continuously decreased, while the amount of F^- adsorbed on the surfaces of solution particles increased, leading to a gradual decrease in zeta potential from −0.9 mV to −7.3 mV as the pH increased from 0.8 to 11.9. In both experiments, the zeta potential decreased as the concentration of F^- ions in the solution decreased.

Figure 15 shows the SEM image of the activated-RM-immobilized PG presented in Figure 8 at pH 8.5, together with the distributions of Fe, Al, F, and P. Fe and Al were evenly distributed and overlapped with the regions enriched in F and P, indicating that the generated amorphous calcium aluminate and calcium ferrite polymers effectively absorbed soluble F and P. Moreover, the experimental results demonstrate that not only does the leachate of PG immobilized with activated RM and $Ca(OH)_2$ meet the environmental requirements (pH = 6–9, P ≤ 0.5 mg/L, F ≤ 10 mg/L), but the F concentration in the leachate also gradually decreased with prolonged storage time.

Figure 16 shows the relationship between the F concentration in the leachate of activated-RM-immobilized PG and storage time. The F concentration decreased from 9.6 mg/L to 5.3 mg/L after one year of storage, indicating that the calcium aluminate and calcium ferrite polymers formed in PG immobilized with activated RM and $Ca(OH)_2$ retained sustained adsorption capacity for soluble F and P. In addition, amorphous materials tend to undergo gradual crystallization over time, as exemplified by crystalline apatite

deposits in southern China that evolved from ancient biological materials [27]. Proper crystallization is known to enhance the performance of fluoride removal materials. Although the XRD patterns of the immobilized PG did not show significant changes after one year, the continuous decrease in F concentration in the leachate suggests that the calcium aluminate and calcium ferrite polymers may have partially crystallized during storage, which is beneficial for long-term environmental protection.

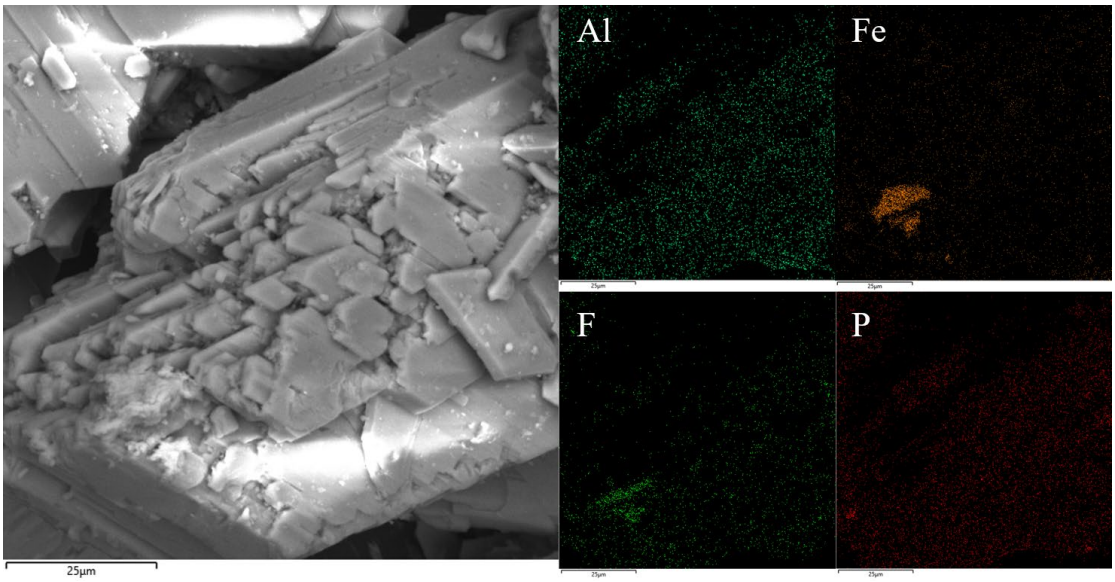


Figure 15. SEM images of RM-immobilized PG and the Fe, Al, F, and P distributions.

The activated RM immobilization process for PG is simple, easy to implement, cost-effective, and exhibits stable and durable performance. During industrial application, site conditions can be flexibly utilized, including rainwater, internal circulating water, and existing water treatment facilities in phosphoric acid plants. The required RM dosage is reduced to only 3% of the PG mass. Therefore, this process has been successfully applied in industry and has achieved favorable results.

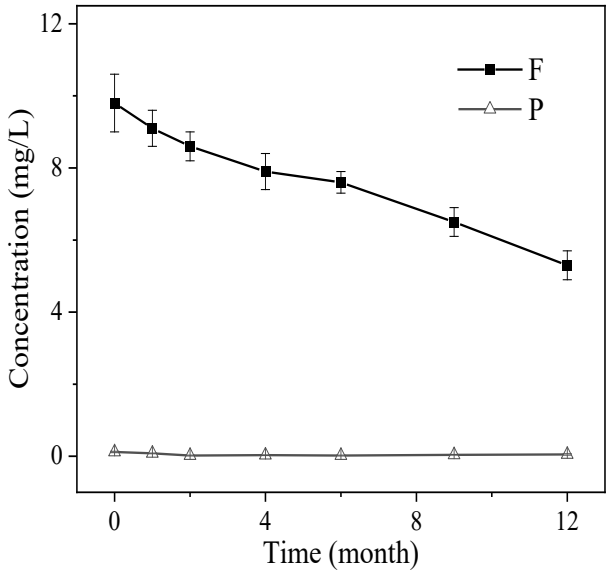


Figure 16. Effect of storage time on the F and P concentration in activated-RM-immobilized PG leachate.

4. Conclusions

This study systematically investigated the washing behavior of soluble phosphorus (P) and fluorine (F) in phosphogypsum and their subsequent immobilization using aluminum- and iron-based compounds as well as sulfuric acid-activated red mud (RM). The results demonstrate that water washing can remove more than 90% of soluble P and F from PG, and lime neutralization can further reduce their concentrations. However, due to the solubility limitations of $CaHPO_4$ and CaF_2, water washing combined with lime neutralization alone cannot reduce the P and F concentrations enough to meet environmental requirements (pH = 6–9, P $\leq$ 0.5 mg/L, F $\leq$ 10 mg/L), indicating that additional immobilization mechanisms are required.

The interaction of soluble Al and Fe species with $Ca(OH)_2$ under ambient conditions leads to the formation of amorphous calcium aluminate and calcium ferrite polymers that act as precursors to crystalline phases. These amorphous polymers exhibit a homogeneous distribution within the PG matrix and provide strong adsorption and fixation sites for soluble P and F, enabling their deep and effective immobilization. This mechanism highlights the importance of amorphous calcium aluminate and calcium ferrite phases in achieving simultaneous P and F stabilization without high-temperature treatment.

Sulfuric acid-activated RM, enriched in soluble Al and Fe, was demonstrated to be an effective and low-cost immobilizing agent. By adding activated RM at only 3 wt.% relative to PG and treating washed PG at a solid–liquid ratio of 1:1 g/mL with $Ca(OH)_2$ adjustment to pH 8.5–9 under stirring, amorphous calcium aluminate and calcium ferrite polymers were uniformly generated. After treatment, the leachate of the immobilized PG contained 0.3 mg/L P and 9.6 mg/L F, meeting the regulatory criteria for general solid waste. Compared with previously reported approaches requiring approximately a 1:1 mass ratio of untreated RM to PG, this method drastically reduces RM consumption while improving the utilization efficiency of Al and Fe.

From an engineering perspective, although sulfuric acid activation is introduced, the overall process remains economically attractive because RM consumption is reduced by an order of magnitude, no high-temperature calcination or mechanical ball milling is required, and the treatment can be implemented under ambient conditions and potentially on-site at PG storage facilities. Moreover, the immobilization products exhibit enhanced long-term stability during stacking, as indicated by the gradual decrease in F concentration over time, suggesting the possible transformation of amorphous phases toward more stable structures. These characteristics confirm the feasibility of a "treating waste with waste" strategy and support the practical application of activated RM for the large-scale, environmentally safe management of phosphogypsum.

Author Contributions: Y.W. (Yi Wang): Conceptualization, Methodology, Software, Formal analysis, Investigation, Data Curation, Writing—Original Draft, Writing—Review and Editing, Visualization, Project administration; Y.W. (Yanhong Wang): Methodology, Validation, Investigation, Resources, Writing—Review and Editing; G.G.: Validation, Investigation, Resources, Writing—Review and Editing; X.W.: Investigation, Resources, Writing—Review and Editing, Funding acquisition. All authors have read and agreed to the published version of the manuscript.

Funding: This work was supported by the National Natural Science Foundation of China (Grant No. 51974369) and NSFC-STINT (Grant No. 52111530192).

Institutional Review Board Statement: Not applicable.

Informed Consent Statement: Not applicable.

Data Availability Statement: All data generated or analyzed during this study are included in this paper.

Conflicts of Interest: The authors declare no conflicts of interest.

References

1. Saadaoui, E.; Ghazel, N.; Ben Romdhane, C.; Massoudi, N. Phosphogypsum: Potential uses and problems—A review. *Int. J. Environ. Stud.* **2017**, *74*, 558–567. [CrossRef]
2. Silva, L.F.O.; Oliveira, M.L.S.; Crissien, T.J.; Santosh, M.; Bolivar, J.; Shao, L.; Dotto, G.L.; Gasparotto, J.; Schindler, M. A review on the environmental impact of phosphogypsum and potential health impacts through the release of nanoparticles. *Chemosphere* **2022**, *286*, 131513. [CrossRef]
3. Wu, F.; Ren, Y.; Qu, G.; Liu, S.; Chen, B.; Liu, X.; Zhao, C.; Li, J. Utilization path of bulk industrial solid waste: A review on the multi-directional resource utilization path of phosphogypsum. *J. Environ. Manag.* **2022**, *313*, 114957. [CrossRef]
4. Ke, H.; Zheng, S.N.; Zhang, P.Z.; Xiao, B.; Lan, J.W.; Zhang, S.; Hu, J. Leaching behavior and release mechanism of pollutants from different depths in a phosphogypsum stockpile. *Waste Manag.* **2024**, *189*, 230–242. [CrossRef]
5. Tayibi, H.; Choura, M.; Lopez, F.A.; Alguacil, F.J.; Lopez-Delgado, A. Environmental impact and management of phosphogypsum. *J. Environ. Manag.* **2009**, *90*, 2377–2386. [CrossRef]
6. Chen, S.; Chen, J.; He, X.; Su, Y.; Jin, Z.; Fan, J.; Qi, H.; Wang, B. Comparative analysis of colloid-mechanical microenvironments on the efficient purification of phosphogypsum. *Constr. Build. Mater.* **2023**, *392*, 132037. [CrossRef]
7. Chen, S.; Chen, J.; He, X.; Su, Y.; Jin, Z.; Wang, B. Micromicelle-mechanical coupling method for high-efficiency phosphorus removal and whiteness improvement of phosphogypsum. *Constr. Build. Mater.* **2022**, *354*, 129220. [CrossRef]
8. Andrade Neto, J.S.; Bersch, J.D.; Silva, T.S.M.; Rodríguez, E.D.; Suzuki, S.; Kirchheim, A.P. Influence of phosphogypsum purification with lime on the properties of cementitious matrices with and without plasticizer. *Constr. Build. Mater.* **2021**, *299*, 123935. [CrossRef]
9. Wu, F.; He, M.; Qu, G.; Zhang, T.; Ren, Y.; Kuang, L.; Ning, P.; Li, J.; Liu, Y. Highly targeted stabilization and release behavior of hazardous substances in phosphogypsum. *Miner. Eng.* **2022**, *189*, 107866. [CrossRef]
10. de Paula, N.; Maraschin, M.; Knani, S.; de Oliveira, J.T.; Agustini, C.B.; Féris, L.A.; Claussen, L.E.; de Souza, D.M.; Oliveira, M.L.S.; Silva, L.F.O.; et al. Ozone-treated activated alumina as an alternative adsorbent to remove fluoride from water: Conventional and Bayesian approaches to evaluate the isotherms, kinetics, and thermodynamics. *J. Environ. Chem. Eng.* **2023**, *11*, 111403. [CrossRef]
11. Peng, W.; Hu, H.; Zhang, Q.; Wang, Y.; Liu, H.; Zhang, X.; Du, X.; Wang, C. Simultaneous immobilizations of soluble phosphorus and fluorine in phosphogypsum by milling with calcareous and aluminiferous samples: Reaction products and immobilization performances. *J. Cleaner Prod.* **2023**, *422*, 138677. [CrossRef]
12. Han, Y.; Qin, Q.; Chang, Q.; Zhang, H.; Zhang, J.; Guan, X.; Xiong, J.; Li, Q.; Tang, J.; Li, G. Investigation of the behavior and mechanism for defluoridation by modified mayenite ($Ca_{12}Al_{14}O_{33}$) in sodium aluminate solution. *Sep. Purif. Technol.* **2025**, *353*, 128412. [CrossRef]
13. Hao, Y. Study on Red Mud Based Calcium Sulphoaluminate Calcium Sulphosilicate—Calcium Ferric Aluminate Cement and Its Properties. Master's Thesis, University of Jinan, Jinan, China, 2022.
14. Gomes, H.C.; Teixeira, S.S.; Graça, M.P.F. Synthesis of calcium ferrite for energy storage applications. *J. Alloys Compd.* **2022**, *921*, 166026. [CrossRef]
15. Koplík, J.; Švec, J.; Másilko, J.; Sedlačík, M.; Bartoníčková, E. Synthesis of calcium aluminate hydrates, their characterization and dehydration. *Ceram. Int.* **2024**, *51*, 5536–5543. [CrossRef]
16. Araújo, M.H.P.; Ardisson, J.D.; Krohling, A.C.; Lago, R.M.; Guimarães Júnior, W.; Tristão, J.C. Calcium ferrites for phosphate adsorption and recovery from wastewater. *RSC Adv.* **2024**, *14*, 1612–1624. [CrossRef]
17. Tsunashima, Y.; Iizuka, A.; Akimoto, J.; Hongo, T.; Yamasaki, A. Preparation of sorbents containing ettringite phase from concrete sludge and their performance in removing borate and fluoride ions from waste water. *Chem. Eng. J.* **2012**, *200–202*, 338–343. [CrossRef]
18. Wang, S.; Chen, Z.; Jiang, H.; Su, J.; Wu, Z. Strength performance and enhancement mechanism of silty sands stabilized with cement, red mud, and phosphogypsum. *J. Build. Eng.* **2023**, *73*, 106762. [CrossRef]
19. Wang, Y.; Liu, B.; Sun, H.; Huang, Y.; Han, G. Selective separation of Al, Fe, and Ti from red mud leachate by Fe-Ti iso precipitate flotation and reduction hydrolysis process: Ions selective chelation and separation mechanism. *J. Environ. Chem. Eng.* **2023**, *11*, 110320. [CrossRef]
20. Hu, Z.; Yao, H. A Method for Reducing Damage to Phosphogypsum and Red Mud, CN101264480A. 2008. Available online: https://d.wanfangdata.com.cn/patent/ChhQYXRlbnROZXdTMjAyNDExMDQxNTI3MzISEENOMjAwODEwMDY4NzI4LjIaCHJpdndzanVp (accessed on 22 January 2026).
21. Agrawal, S.; Dhawan, N. Process flowsheet for extraction of Fe, Al, Ti, Sc, and Ga values from red mud. *Miner. Eng.* **2022**, *184*, 107601. [CrossRef]
22. Zinoveev, D.; Pasechnik, L.; Fedotov, M.; Dyubanov, V.; Grudinsky, P.; Alpatov, A. Extraction of Valuable Elements from Red Mud with a Focus on Using Liquid Media—A Review. *Recycling* **2021**, *6*, 38. [CrossRef]
23. Zhao, M.; Li, X.; Yu, J.; Li, F.; Guo, L.; Song, G.; Xiao, C.; Zhou, F.; Chi, R.; Feng, G. Highly efficient recovery of phosphate and fluoride from phosphogypsum leachate: Selective precipitation and adsorption. *J. Environ. Manag.* **2024**, *367*, 122064. [CrossRef]

24. Yatsenko, D.A.; Pakharukova, V.P.; Tsybulya, S.V. Low Temperature Transitional Aluminas: Structure Specifics and Related X-ray Diffraction Features. *Crystals* **2021**, *11*, 690. [CrossRef]
25. Zhang, J.; Tian, C.; Xu, Y.; Chen, J.; Xiao, L.; Wu, G.; Jin, F. Effective removal of fluorine ions in phosphoric acid by silicate molecular sieve synthesized by hexafluorosilicic acid. *Sep. Purif. Technol.* **2023**, *305*, 122395. [CrossRef]
26. Speight, J. *Lange's Handbook of Chemistry*; McGraw-Hill: New York, NY, USA, 2005.
27. Peng, R.; Yang, R.; Chen, J.; Gao, J.; Gao, L.; Gao, C. Biogenic mineralization controls exceptional REY enrichment in Early Cambrian phosphorites from South China. *Ore Geol. Rev.* **2025**, *178*, 106497. [CrossRef]

Disclaimer/Publisher's Note: The statements, opinions and data contained in all publications are solely those of the individual author(s) and contributor(s) and not of MDPI and/or the editor(s). MDPI and/or the editor(s) disclaim responsibility for any injury to people or property resulting from any ideas, methods, instructions or products referred to in the content.